MASERS IN STAR-FORMING REGIONS

N. D. KYLAFIS
University of Crete
Physics Department
P.O. Box 2208
710 03 Heraklion, Crete
Greece

AND

K. G. PAVLAKIS
University of Leeds
Department of Physics and Astronomy
Woodhouse Lane
Leeds LS2 9JT
United Kingdom

1. Introduction

The subject of astronomical masers is now more than forty years old, and as a consequence, several good reviews have appeared in print. For the readers who want to enter the subject of astronomical masers in a serious way, we want to recommend two reviews (Elitzur 1982; Reid and Moran 1988) and a book (Elitzur 1992a). They contain reviews of the observations as well as the basic ideas and equations that will enable the readers to comprehend the research papers on the subject. The most recent review in the Annual Reviews of Astronomy and Astrophysics is that of Elitzur (1992b).

In the present review, we want to avoid the mathematical details but stress instead a qualitative understanding of astronomical masers. Needless to say, some overlap with the above reviews is unavoidable. Section 2 contains the basic concepts regarding masers. In §3 the differences between laboratory and astronomical masers are briefly discussed and in §4 a few examples which demonstrate the usefulness of astronomical masers are presented. Section 5 describes what it takes to build a maser model and how well we know the various input parameters. The observations and proposed

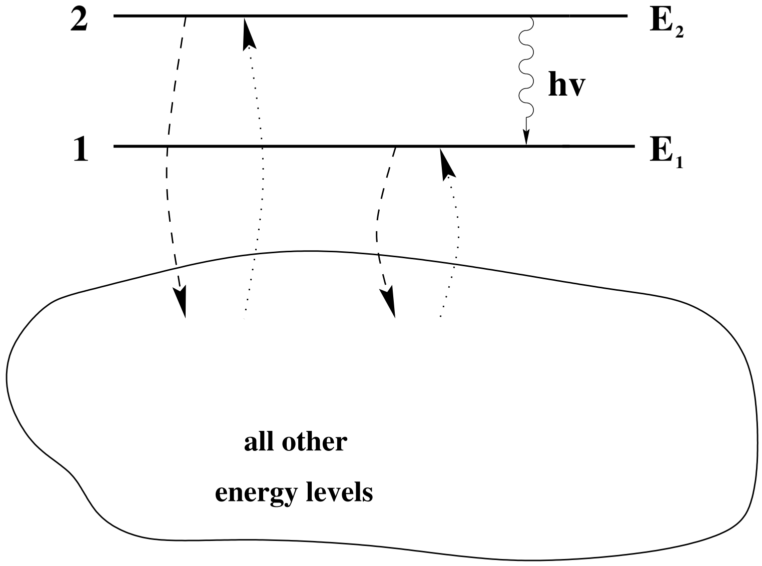

Figure 1. *Schematic energy level diagram of a molecule. Only two levels are explicitly shown. The rest are lumped together and are considered as a reservoir. The dotted and dashed arrows indicate respectively the transitions from the reservoir to the two levels and the opposite.*

pumping mechanisms are given in §6 for OH and H_2O masers. The location of OH and H_2O masers in star-forming regions is discussed in §7 and the conclusions are given in §8.

2. Basic Concepts

The energy level diagram of a molecule consists of an infinite number of levels. Nevertheless, one need only consider a finite and relatively small number of energy levels in order to perform an accurate model calculation regarding a specific molecule. Even better, for the purposes of a qualitative discussion of masers, one can consider only two energy levels and treat the rest of them as a reservoir. Figure 1 shows such a simplified model of a molecule.

Level 1 is the lower maser level and level 2 is the upper one. The energy difference between the two levels is $\Delta E \equiv E_2 - E_1 = h\nu$, where ν is the frequency of the maser. Collisional and radiative transitions cause the molecules to circulate between the reservoir and the maser levels. Thus, the dotted lines in Figure 1 indicate the transitions of molecules from the reservoir to the maser levels. The opposite transitions are indicated by dashed lines. Let n_1 and n_2 be the populations *per magnetic sublevel* of the two maser levels. The maser phenomenon occurs if, in steady state, the populations satisfy the condition $n_2 > n_1$. This is because, as a photon of frequency ν propagates, it is more likely to cause stimulated emission than to be absorbed.

2.1. AMPLIFICATION

Consider radiation of frequency ν and intensity I propagating through molecules whose energy level diagram is that of Figure 1. The change dI in the intensity that occurs as the radiation propagates by a length dl through the medium is

$$dI = -\kappa I dl \ , \tag{1}$$

where $\kappa \propto (n_1 - n_2)$ is the absorption coefficient corrected for stimulated emission. Here it is assumed for simplicity that the molecules do not emit radiation by spontaneous emission. Defining the optical depth τ by $d\tau \equiv \kappa dl$, one finds that the intensity as a function of optical depth is given by

$$I = I_0 e^{-\tau} \ , \tag{2}$$

where I_0 is the intensity of a background source that is incoming to the medium. If the populations of levels 1 and 2 in Figure 1 are such that $n_1 > n_2$, then $\tau > 0$ and the radiation is attenuated as it propagates through the medium. This situation is typical in astronomical environments and it leads to the formation of absorption lines. On the other hand, if $n_1 < n_2$, the optical depth is negative and the radiation is amplified. This is because a propagating photon is more likely to cause a stimulated emission than it is to be absorbed. Thus, one photon leads to two propagating in the same direction, two photons to four and so on. In other words, the amplification of the radiation is *exponential*.

As mentioned above, it was only for simplicity that spontaneous emission in the medium was neglected. In reality, such an emission always occurs and the radiation thus produced is also amplified. If there is no background source, as it is the case in most astronomical masers, it is only the spontaneous emission that gets amplified.

2.2. SATURATION

The exponential growth of the radiation intensity in a medium that exhibits inverted populations is truly fascinating. It is therefore important to investigate whether this exponential growth has any limits, assuming that the maser region is long enough. Since a stimulated emission event causes the transition of a molecule from the upper maser level to the lower, it is clear that stimulated emission tends to *reduce* the population inversion. At low intensities, the stimulated emission rate is relatively small and the population difference $n_1 - n_2$ remains essentially unaffected. As the intensity grows, so does the stimulated rate. Thus, a point is reached where the stimulated emission rate becomes comparable to the rate that causes the population inversion. At this point, *saturation* has set in because the rate of extraction of photons has reached its limiting value, which is the pumping rate (the rate of population inversion). Increasing the volume of the emission region under saturation conditions will only increase the photon emission rate in proportion to the volume.

It is important to remark here that the astronomical definition of *saturation* given above is exactly opposite to that used by experimental physicists for laboratory masers and lasers. Experimental physicists call a maser *saturated* when its intensity grows exponentially.

2.3. THERMALIZATION

The establishment of inverted populations in a medium containing a certain kind of molecules is not as difficult as one might think. In fact, it is not an exaggeration to say that if the molecules are abused, they will most likely exhibit inverted populations in *some pair* of energy levels. One cannot easily predict which pair it will be, but inversion in some pair is almost certain. Common methods of abuse of molecules in astronomical environments are a) collisions with other molecules, b) irradiation of the molecules and c) a combination of the above, which is the usual case. As an illustration, let us consider collisions with other molecules (e.g., H_2) as the cause of population inversion. If the density of H_2 molecules is low, the collision rate is low, the rate of population inversion is low and therefore the maser luminosity is correspondingly low. For low rates of abuse, the maser luminosity increases in proportion to the rate of abuse of the molecules. However, this proportionality has an upper limit. When the collision rate becomes very large, the collisional transitions of the molecules dominate all other transitions (see § 5.3 below), the molecules thermalize at the temperature of the H_2 molecules and the population inversion is destroyed. At thermalization, the level populations obey the Boltzmann distribution, namely

$$\frac{n_2}{n_1} = \exp(-\Delta E/kT) < 1 \ , \tag{3}$$

where T is the temperature of the H_2 molecules.

2.4. BEAMING

The majority of the astronomical masers *do not* emit isotropically. This effect can be understood as follows: Consider a maser region which is not spherically symmetric but instead it is elongated in some direction, as shown

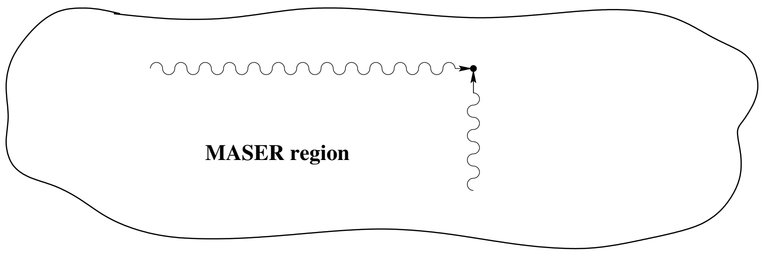

Figure 2. *Schematic representation of a maser region. The two wiggly arrows indicate the intensity of the maser in two directions.*

in Figure 2. The gain $|\tau|$ along the direction of elongation is larger than in directions perpendicular to it. Consequently, the intensity of the maser is largest along the direction of elongation. Thus, a departure from spherical symmetry introduces an anisotropy in the intensity.

Once an anisotropy in the intensity is established, it is further enhanced through the following process. Consider the maser photons that reach a certain point in the maser region from all possible directions (see Figure 2). These beams of photons compete for the available pump photons there. The rate of stimulated emission caused by a given beam is proportional to its intensity. Therefore, the stronger beam wins and becomes even stronger (Alcock and Ross 1985a,b; 1986). As a result, a non-spherically symmetric maser region results in maser emission in two opposite cones along the direction of elongation.

Radio observers measure the flux of photons that reach their telescope and, not knowing the degree of beaming, make the assumption that the emission is isotropic. Thus, from the observed flux, an equivalent *isotropic* luminosity is quoted for the source. This procedure certainly overestimates the luminosity of a *maser spot*, but it gives the right value when one considers a region that contains many maser spots. This is because the cones of emission of the various spots have random orientations, but we only see the ones that are directed towards the earth.

2.5. GEOMETRY AND APPARENT SIZE

The geometry of a maser region and its apparent size are intimately related. Furthermore, the apparent size of a maser region may be significantly smaller than its actual size. For the purposes of illustration we will consider two shapes of maser region, elongated and nearly spherical.

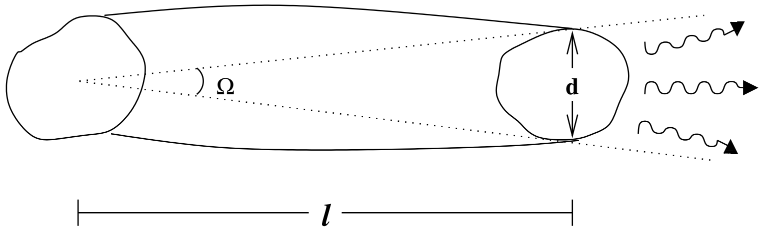

Figure 3. *Schematic of a maser region which is approximately cylindrical. The wiggly lines indicate the emergent maser intensity.*

2.5.1. *Elongated Structures*

Consider a maser region which is more or less cylindrical as shown in Figure 3. Let the length of the region be l and its characteristic width be d, with $l \gg d$. As discussed in § 2.4, most of the maser photons escape through the bases of the cylinder and into solid angles $\Omega \sim (d/l)^2$.

If the observational direction falls in this beaming angle Ω, then the observer sees the maser spot and determines an apparent size $\sim d$. If, on the other hand, the observational direction falls significantly outside Ω, the observer *does not* see the maser spot, because the intensity of the maser in the direction of the observer is below the detection limit.

2.5.2. *Nearly Spherical Structures*

Consider now a maser region which is nearly spherical with diameter D, as shown in Figure 4. In this case, all observers see the maser spot as having the same apparent size. However, the apparent size is *less* than D because the rays that come out of the region have traversed different lengths and therefore the maser photons have experienced different gains. It is straightforward to estimate the apparent size of the maser spot once the detection limit of the telescope is given.

2.6. VARIABILITY

All masers, even the very strong ones, are variable (see, e.g., Clegg and Cordes 1991; Lekht, Mendoza-Torres and Sorochenko 1995; Claussen *et al.* 1996). This, of course, is not surprising because even a small change in the gain introduces a significant change in the intensity. Small changes in the gain can be caused either by changes in the aspect angle or by changes in the local physical parameters such as the density and the velocity field. For example, if the maser region is elongated, a small change in the aspect angle may result in a relatively large change in the intensity (see § 2.5.1).

Despite the short timescale of variability, some maser spots can be followed for years. The lifetime of individual spots can be as large as one to

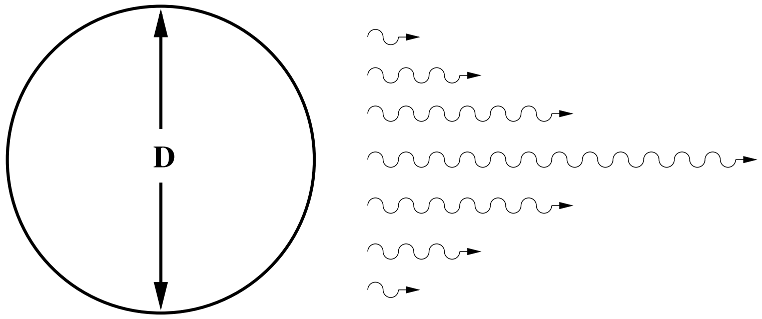

Figure 4. *Schematic of a maser region which is approximately spherical. The wiggly lines indicate the emergent maser intensity.*

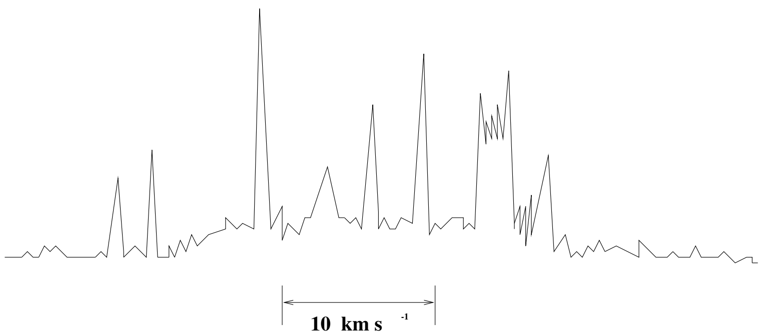

Figure 5. *A sketch of a spectrum of* H_2O *emission in a region of star formation.*

two years for H_2O and more than ten years for OH masers. This relatively long lifetime has allowed studies of proper motion of the maser spots and through this the determination of their distance (see § 4).

2.7. SPECTRA AND LINE WIDTHS

The maser spectra observed in star-forming regions are fairly complex (see Genzel and Downes 1977 for a collection of such spectra). A sketch of a typical spectrum of H_2O emission in a region of star formation is shown in Figure 5.

H_2O maser spectra in star-forming regions extend over a frequency range corresponding to a velocity difference of a few tens km s^{-1} (typically less than 10 km s^{-1} for OH) and consist of many spikes. VLBI maps which resolve the maser region have shown that a spike arises from one or more distinct spots. The line width of a strong spike is typically a few times smaller than the width expected from the thermal motions of the molecules. This is expected because unlike a thermal line, a maser line grows exponentially (in the unsaturated regime) and therefore the full width at half maximum is smaller than thermal. As the line center saturates, the line wings continue to grow exponentially and the line width approaches the thermal one.

The reader should not be left with the impression that unsaturated lines have narrow widths while saturated ones have thermal widths. It has been demonstrated by Goldreich and Kwan (1974) that the broadening of the line during saturation can be inhibited if trapping of the infrared radiation involved in the pumping occurs.

2.8. POLARIZATION

Polarization is fairly common in masers observed in star-forming regions. The OH masers are typically highly polarized while the H_2O ones show polarized features in about 25% of the sources. In order for a maser source to emit polarized radiation, the molecules must not only exhibit inverted populations but also unequal populations in the magnetic sublevels. It has been demonstrated (Goldreich, Keeley and Kwan 1973) that an ordered magnetic field in the maser region can establish unequal populations in the magnetic sublevels and therefore result in polarized emission. The magnetic field required is of order a few milligauss for OH and somewhat larger for H_2O.

The maser polarization would be an ideal way of measuring the magnetic field strength in maser regions if the magnetic field were the only cause of such polarization. As it has been demonstrated (Western and Watson 1983a,b,c, 1984; Deguchi and Watson 1986a,b; Deguchi, Watson and Western 1986; Deguchi and Watson 1990; Nedoluha and Watson 1990a,b,c; Elitzur 1991, 1993; Watson 1994; Nedoluha and Watson 1994; Elitzur 1995, 1996; Wallin and Watson 1997), anisotropic radiation fields in the maser region can also cause polarization. Thus, the origin of the observed polarization is not always clear.

Despite the above ambiguity, the unmistakable Zeeman pattern has been seen by Moran *et al.* (1978) for OH and Fiebig and Güsten (1989) for H_2O. These observations have determined the magnetic field strength to be 2 to 9 milligauss in W3(OH) and of order 50 milligauss in Orion KL and W49N.

The Zeeman splitting of OH maser lines can also yield the line-of-sight direction of the magnetic field. Reid and Silverstein (1990) have in this way been able to infer the direction of the magnetic field in maser sources over large regions of the Galaxy.

3. Laboratory versus Astronomical Masers

Both laboratory and astronomical masers are based on the same principle, namely, some transition exhibits inverted populations. Nevertheless, there are significant differences in the size and the technical characteristics of the two.

In laboratory masers, the maser region is typically $\sim$ 1 m long (to astronomical accuracy). In order to have significant gain, the radiation is bounced between two mirrors, one of which is semi-transparent to allow the amplified radiation to escape. On the other hand, the astronomical masers have significantly lower densities but gain lengths of order a few AU or larger. The absence of reflecting boundaries in astronomical masers makes them single pass as opposed to multi pass in the laboratory ones. Furthermore, the fixed size of the laboratory masers introduces a mode selection, i.e., not all wavelengths can fit in the length of the maser. On the other hand, the astronomical masers allow all possible wavelengths and they are broad band. Finally, laboratory masers emit coherent radiation, while the astronomical ones emit non-coherent. This is because in astronomical masers the beaming angle (see § 2.4) is fairly large and therefore a significant phase difference is introduced between two rays in the beam.

Because the radiative transfer in astronomical masers is relatively simple (see § 5), the main theoretical effort has concentrated on inventing efficient pumping mechanisms and understanding the origin of polarization.

4. Usefulness of Masers

The astronomical masers, because of their unique properties, provide very useful information. Below are listed some of the most important results that have been obtained from maser observations.

As mentioned in § 2.8, when a maser line shows the Zeeman pattern, the magnetic field in the maser region is determined unambiguously. Thus, we now have an accurate knowledge of the magnetic field strength in some OH and H_2O maser regions.

Observations of maser spots have provided detailed information on the dynamics of a region. As an interesting example, we mention the work of Chapman and Cohen (1986, see their Figures 5 and 6), who studied OH and H_2O maser emission from the circumstellar envelope of the supergiant star VX Sagittarius and inferred the velocity field there.

VLBI proper motion studies of H_2O maser spots have provided a means to determine distances across the Milky way. Thus, the distances to Orion KL and W51(Main) have been determined to be respectively 480 ± 80 pc (Genzel *et al.* 1981a) and 7.0 ± 1.5 kpc (Genzel *et al.* 1981b). The distance to W51(North) is 7 ± 2 kpc (Schneps *et al.* 1981), the distance to Sgr-B2(North) is 7.1 ± 1.5 kpc (Reid *et al.* 1987) and the distance to W49N is 11.4 ± 1.2 kpc (Gwinn, Moran and Reid 1992).

The long-standing problem of locating the position of the compact non-thermal radio source Sgr A* on infrared images of the Galactic center region has been solved with the use of maser observations (Menten et al. 1997).

The astronomical masers can also be useful on earth. The brightest maser source in the sky (Orion KL) has been used in a holographic technique to measure the figure of large radio telescopes (Moran 1989).

With the development in maser modeling, we are now in a position to infer physical conditions in star-forming regions from observations of all the maser lines exhibited by a molecule (Kaufman and Neufeld 1996; Pavlakis and Kylafis 1996b,c; 1999).

Submilliarcsecond VLBI mapping of the H_2O maser emission in NGC 4258 has shown that the masers are located in a thin disk around the central black hole (Miyoshi *et al.* 1995). It is the first time that we see structure [probably a warped disk (Herrnstein, Greenhill and Moran 1996)] at a distance of 0.2 pc from the central black hole of an AGN.

5. Maser Models

In what follows, the requirements for the construction of a maser model are discussed and the basic equations that need to be solved are given. Also, a qualitative discussion of how collisional and radiative pumping works is presented.

5.1. REQUIREMENTS

In order to construct a maser model one needs the following:

a) The energy levels of the molecule that exhibits maser emission. These are generally well known.

b) The einstein coefficients A_{ij} for the transitions from any upper level i to any lower level j. These also are well known, at least for the most common molecules.

c) The collision rates C_{ij} for transitions from any level i to any level j of the maser molecule. The colliding particles are the other molecules in the region (e.g., H_2). These rates are only approximately known. Therefore, when maser models are constructed, it should always be kept in mind that the currently published collision rates may be revised.

d) The velocity field in the maser region. This is unknown and it is only guessed in maser models. Two types of velocity field have generally been assumed. In one, the medium is static and the molecules obey a distribution of velocities (typically Gaussian). In the other, the medium exhibits a large velocity gradient, i.e., the macroscopic velocity differences are significantly larger than the thermal velocities of the molecules.

e) The geometry of the maser region is also unknown and in maser models a simple (typically spherical or cylindrical) geometry is assumed.

5.2. BASIC EQUATIONS

The set of equations that need to be solved consists of the statistical equilibrium equations for the level populations and the radiative transfer equations for the various line frequencies. For simplicity, we will assume that the molecules under study have only three, non-degenerate energy levels with energies E_1, E_2 and E_3 and corresponding populations n_1, n_2 and n_3. If only collisional and radiative transitions are taken into account, the steady state equations describing the level populations are

$$\frac{dn_3}{dt} = -(A_{32} + A_{31})n_3 + R_{13}(n_1 - n_3) + R_{23}(n_2 - n_3)$$

$$+C_{13}n_1 + C_{23}n_2 - (C_{32} + C_{31})n_3 = 0 \ , \qquad (4a)$$

$$\frac{dn_2}{dt} = A_{32}n_3 - A_{21}n_2 - R_{23}(n_2 - n_3) + R_{12}(n_1 - n_2)$$

$$+C_{12}n_1 + C_{32}n_3 - (C_{23} + C_{21})n_2 = 0 \ , \qquad (4b)$$

$$n_1 + n_2 + n_3 = N \ , \qquad (4c)$$

where N is the total number of maser molecules and R_{ij} are the radiative absorption rates corrected for stimulated emission. Generalization of these equations to any number of levels is straightforward.

If ν is the frequency of the transition from upper level j to lower level i and I_ν is the corresponding intensity, then the radiative transfer equation is given by

$$\frac{dI_\nu}{dl} = -\kappa_\nu I_\nu + \eta_\nu \ , \qquad (5)$$

where κ_ν is the absorption coefficient (which is a function of ν and $n_i - n_j$) and η_ν is the emissivity (which is a function of ν and n_j).

The system of equations (4) and (5) must be solved simultaneously (Goldreich and Keeley 1972; Elitzur 1990a,b). In the case where there is a large velocity gradient in the medium, equations (4) and (5) are decoupled (Sobolev 1960; Castor 1970). For a complete formalism in this case see, for example, Kylafis and Norman (1991).

5.3. COLLISIONAL AND RADIATIVE PUMPING

Collisional pumping works as follows: The maser molecules are excited by collisions with the other particles (typically H_2) in the maser region. Their de-excitation is done both radiatively and collisionally. If the radiative de-excitations dominate the collisional ones, it is likely that some transition will exhibit inverted populations. However, when the collisions dominate both excitations and de-excitations, the molecules thermalize and the population inversion is destroyed. Equations (4), with only collision terms, yield the Boltzmann distribution for the level populations.

Radiative pumping works in a similar way. The excitation of the molecules is done with infrared radiation from an external source. The de-excitation is done via spontaneous and stimulated emission. In this "flow" of the molecules from level to level, it is likely that inverted populations will be established in some transition. If the external radiation dominates in the de-excitation, thermodynamic equilibrium is established at the temperature of the external radiation.

6. Masers in Star-Forming Regions

Maser emission is a common phenomenon in star-forming regions. The best studied masers in such regions are the OH and H_2O ones. In recent years, the methanol and the ammonia masers have received a lot of attention. The SiO masers are rare (they have been seen only in Orion, W51 and Sgr B2), while other molecules exhibit fairly weak maser emission.

Here we will concentrate on the OH and the H_2O masers in star-forming regions.

6.1. OH MASERS

The energy levels of OH are grouped into two ladders, the $^2\Pi_{3/2}$ and the $^2\Pi_{1/2}$ (see, e.g., Figure 1 of Pavlakis and Kylafis 1996b for an energy level diagram). In each ladder, the energy levels are characterized by the total angular momentum J and are split into Λ-doublets. Each component in a given Λ-doublet is further split into two hyperfine levels. Thus, there are four allowed ground state transitions and many excited ones in the $^2\Pi_{3/2}$ and $^2\Pi_{1/2}$ ladders.

The OH molecules in star-forming regions are rich in maser emission. They exhibit four maser lines (at 18 cm) in the ground state $^2\Pi_{3/2}$, $J = 3/2$ (e.g., Gaume and Mutel 1987; Cohen, Baart and Jonas 1988), three maser lines (at 5 cm) in the first excited state $^2\Pi_{3/2}$, $J = 5/2$ (Knowles, Caswell and Goss 1976; Guilloteau et al. 1984; Smits 1994; Caswell and Vaile 1995; Baudry et al. 1997; Desmurs et al. 1998; Desmurs and Baudry 1998), three maser lines (at 6 cm) in the next level $^2\Pi_{1/2}$, $J = 1/2$ (Gardner and Martin Pintado 1983; Gardner and Whiteoak 1983; Palmer, Gardner and Whiteoak 1984; Gardner, Whiteoak and Palmer 1987; Baudry et al. 1988; Baudry and

Diamond 1991; Cohen, Masheder and Walker 1991) and one maser line (at 2 cm) in the level $^2\Pi_{3/2}$, $J = 7/2$ (Turner, Palmer and Zuckerman 1970; Baudry et al. 1981; Baudry and Diamond 1998).

The four transitions in the ground state are the best known ones. They have wavelengths approximately 18 cm and frequencies 1665, 1667 MHz (main lines) and 1720, 1612 MHz (satellite lines).

6.1.1. *Observations*

From the extensive observational study of star-forming regions by Gaume and Mutel (1987), the following observational characteristics have appeared.

a) All four ground-state transitions of OH have been seen as masers (not all four, though, from the same maser spots).

b) The main-line masers at 1665 and 1667 MHz are usually the most common masers with the intensity of the 1665 MHz line typically larger than the intensity of the 1667 MHz line.

c) Most (but not all) of the 18 cm masers are found at the projected edges of H II regions.

d) The observations *do not support* a simple shell model for the OH maser distribution.

e) VLBA observations of the excited-state 13.4 GHz maser in W3(OH) with spatial resolution 670 μarcsec (Baudry and Diamond 1998) reveal that no simple geometry exists for the individual maser spots. Perhaps they are related with local shocks.

f) No correlation has been found between the fluxes of individual features and their distances from the centers of the H II regions.

g) Proper motion studies (Bloemhof, Reid and Moran 1992; Migenes, Cohen and Brebner 1992; Bloemhof, Moran and Reid 1996) show motion *away* from the central H II regions.

For some time, the observations of OH masers were way ahead of the theoretical interpretation. For example, in W3(OH) *all* radio transitions between rotational states below 510 K had been observed (for a summary see Table 1 of Cesaroni and Walmsley 1991). They include nine maser lines and twelve emission or absorption ones. In the review of Reid and Moran (1981, see their Table 1), one can see that several OH maser lines have been seen in tens of sources. Also, correlations between ground and excited state masers have been observed (Gardner, Whiteoak and Palmer 1987; Baudry et al. 1988; Cohen, Masheder and Walker 1991). Fortunately, the situation has changed recently (see below) and now the theoretical calculations can be used as diagnostics of the physical conditions in star-forming regions.

6.1.2. *Theoretical calculations*

Before discussing the latest developments on our understanding of the OH masers, we will give a brief account of the various attempts that were made to explain the ground state OH masers.

An attractive suggestion by Andresen (1986) that the 18 cm OH masers are pumped by photodissociation of H_2O is ruled out. This is because the H_2O has to be reformed at a rate which is larger than the collision rate. This is not possible.

The work of Kylafis and Norman (1990) showed that the ground state OH masers *are not* pumped by collisions alone.

Model applications to H II/OH were performed by Cesaroni and Walmsley (1991), Gray, Doel and Field (1991) and Gray, Field and Doel (1992) using both collisional and radiative excitation of OH, and taking into account radiative trapping and line overlap. Cesaroni and Walmsley (1991) succeeded, with some combination of the parameters of their model, to reproduce qualitatively the observed lines of OH for the best studied star forming region W3(OH). This was very encouraging for further detailed studies of OH masers in star-forming regions. The work of Gray, Doel and Field (1991) and Gray, Field and Doel (1992) is quite extensive, but it is a pity that the collision rates they used were outdated and the new ones are so different that qualitatively different conclusions are introduced in some cases. Also, their treatment of line overlap is not sound, because the formulae they have used are unproven.

In view of the wealth of available data and the recently calculated collision rates between OH and H_2, we undertook a systematic study of OH maser pumping in star-forming regions with the hope that we will be able to invert (at least partially) the maser problem. We added one pumping mechanism at a time (collisions, local line overlap, non-local line overlap, external infrared radiation field) and explored the various parameter regimes for each combination of pumping mechanisms.

Our work was an improvement over the work of previous researchers in two main aspects. First, we treated local and non-local line overlap with the use of the recently developed formalism (Pavlakis and Kylafis 1996a). Previous workers have either assumed complete (i.e., 100%) line overlap (Cesaroni and Walmsley 1991) or treated line overlap in a heuristic, unproven way (Doel, Gray and Field 1990; Gray, Doel and Field 1991; Gray, Field and Doel 1992).

Second, we used the recently calculated collision rates between OH and H_2 (Offer, van Hemert and van Dishoeck 1994) and for the first time we distinguished between ortho-H_2 and para-H_2. All previous calculations considered para-H_2. As we found out, it makes a big difference in which form H_2 is in the interstellar medium. It is thus hoped that our work will help distinguish between the two forms of H_2 in maser regions and help determine the abundance of ortho-H_2.

The results of our calculations appeared in Pavlakis and Kylafis (1996b,c) and our major conclusion was that with reasonable values of the parameters it was possible to explain the general characteristics of the 18 cm and the 6 cm OH masers. In addition, with our exploration of the parameter regimes, we were able to propose a number of diagnostics of the physical conditions in star-forming regions using maser observations. For example, if both the 1665 MHz and the 1667 MHz maser lines are seen *in the same spatial region*, then a far infrared radiation field must be present and the density must be less than or of order 10^6 cm^{-3} there.

In our study of the OH maser pumping we had also computed the maser emission of the 5 cm lines of OH, but we decided to not show or discuss the maser lines in the excited state $^2\Pi_{3/2}$, $J = 5/2$, because this state is directly connected with the state $^2\Pi_{1/2}$, $J = 7/2$, which was not included in our calculations. The omission of this state could, in principle, affect the results.

Soon after our calculations were published, Baudry et al. (1997) reported an extensive study of the 5 cm maser lines of OH in star-forming regions. To our surprise, *our already performed calculations explained the observed characteristics.* This probably means that, for temperatures between 100 and 200 K that are thought appropriate for OH maser regions, the missing collision rates are not important for the 5 cm masers. Thus, now we can claim that the essential observational characteristics of the 18 cm, the 6 cm and the 5 cm OH masers in star-forming regions can all be explained with the same set of reasonable values of the parameters (Pavlakis and Kylafis 1999). Of course, when the missing collision rates are computed, it will be reassuring to show that they are indeed not important for the 5 cm masers.

6.2. H_2O MASERS

The rotational energy levels of H_2O are characterized by three quantum numbers and are denoted by $J_{K_+K_-}$, where J is the total angular momentum and K_+ and K_- are its projections on two molecular axes. For an energy level diagram of H_2O see, e.g., Neufeld and Melnick (1991).

The first H_2O maser transition was detected thirty years ago (Cheung *et al.* 1969). It is the transition from level 6_{16} to level 5_{23}, giving rise to radiation with frequency $\nu = 22$ GHz or wavelength $\lambda = 1.35$ cm. This transition lies 640 K above the ground state.

6.2.1. *Observations*

Up to 1990, the words H_2O masers were synonymous with the transition at 22 GHz. In 1990, three mm lines were reported as masers. These are: $10_{29} - 9_{36}$ at 321 GHz (Menten, Melnick and Phillips 1990), $3_{13} - 2_{20}$ at 183 GHz (Cernicharo *et al.* 1990) and $5_{15} - 4_{22}$ at 325 GHz (Menten *et al.* 1990). Of these, the 321 GHz transition lies 1860 K above the ground state. Therefore, it is likely that this transition is excited in a warm (say, 1000 K) environment. Three years later, three sub-mm maser lines were observed (Melnick *et al.* 1993). These are: $7_{53} - 6_{60}$ at 437 GHz, $6_{43} - 5_{50}$ at 439 GHz and $6_{42} - 5_{51}$ at 471 GHz.

Water maser emission is a common feature of deeply embedded young stellar objects (YSOs). It must be stressed though, that H_2O maser emission *does not guarantee* that star formation is taking place there.

It is now widely accepted that the H_2O masers occur in shocks and that the pumping is collisional.

6.2.2. *Theoretical Calculations*

As with the OH masers, we will give a brief account of the attempts to explain the H_2O masers in star-forming regions.

Radiative pumping of the H_2O masers can be ruled out because, even with 100% efficiency, one infrared pumping photon is needed for every maser photon emitted. However, the observed number of infrared pumping photons is significantly lower than the observed maser photons.

Collisions with H_2 molecules on the other hand *can* invert the 22 GHz transition (Elitzur, Hollenbach and McKee 1989; Kylafis and Norman 1991) as well as the three mm transitions (Neufeld and Melnick 1990; 1991) and the three sub-mm ones (Kaufman and Neufeld 1996). The detected transitions, as well as a few more that will undoubtedly be detected in the near future, will constrain the models significantly.

Strelnitskij (1984) proposed the very interesting idea that the H_2O molecules collide with two kinds of particles (e.g., H_2 and electrons) at different kinetic temperatures, but with comparable collision rates. In other words, the H_2O molecules find themselves in contact with two heat baths, and not knowing which of the two Maxwellian distributions to obey, they obey none. Thus, even at very high densities the H_2O molecules are not thermalized. Kylafis and Norman (1986; 1987) showed that, with the then available collision rates, collisional pumping of H_2O in environments where the temperature of the neutral particles is significantly less than that of the electrons, *can* sustain inverted populations. Such environments exist in the magnetic precursors of MHD shocks (Draine, Roberge and Dalgarno 1983; Kaufman and Neufeld 1996).

This idea is now temporarily abandoned because the recalculated collision rates (Palma *et al.* 1988) are significantly different than the older ones. Anderson and Watson (1990) have shown that with the new rates inversion does not occur.

Elitzur, Hollenbach and McKee (1989) proposed that all H_2O masers in star-forming regions, even the very powerful ones, can be explained with conventional collisional pumping. They modeled the maser regions as static, in the shape of cylinders with aspect ratios (see Figure 3) $10 \lesssim l/d \lesssim 100$. This is fine, but it is a little difficult to imagine how such long and narrow structures can exist in star-forming regions. Furthermore, if there is a velocity gradient $\Delta v/l \gtrsim \Delta v_{thermal}/l$ along the axis of the cylinder (which is not unreasonable), then the gain is lower and one needs aspect ratios $l/d > 100$ to explain the powerful H_2O masers (Kylafis and Norman 1991).

An interesting idea regarding the powerful H_2O masers was proposed by Deguchi and Watson (1989). Consider two cylindrical masers, of length l and base diameter d each, separated by a distance D and having their axes aligned. The observer is located on their common axis. If there were only one maser, its radiation would be beamed into a solid angle $\Omega \sim (d/l)^2$ (see § 2.4). However, the radiation of the back maser causes by stimulated emission the radiation of the front maser to be emitted in a much smaller solid angle $\Omega \sim (d/D)^2$. Thus, the observer detects radiation that would not be detected if the front maser emitted its radiation into $\Omega \sim (d/l)^2$. The aligned masers do not emit more than their sum, but *they give you the impression of a powerful maser.* A quantification of this effect was made by Kylafis and Pavlakis (1992).

All the previous model calculations addressed the 22 GHz H_2O maser line and included energy levels up to about $E/k = 1000$ K. For the 321 GHz line, energy levels up to about $E/k = 7000$ K had to be included (Neufeld and Melnick 1991; Kaufman and Neufeld 1996). These impressive calculations explain not only the pumping of all the observed H_2O maser lines, but they also predict that more maser transitions should be seen.

7. Location of Masers

Significant progress has been made in the last few years in pinpointing the positions of masers close to the YSO (e.g., Torrelles *et al.* 1996; Fiebig *et al.* 1996; Hofner and Churchwell 1996; Meehan *et al.* 1998; Torrelles *et al.* 1998) and in associating the positions of the masers with the evolutionary state of the YSO.

Through extensive surveys, the group in Firenze and others showed that most of the H_2O masers (up to 80%) are not associated with diffuse H II regions (Palla *et al.* 1993). Instead, it was shown that the H_2O masers trace the earliest evolutionary phases of massive stars (Codella *et al.* 1994; Palumbo *et al.* 1994; Codella and Felli 1995; Codella *et al.* 1995; Codella, Felli and Natale 1996; Codella, Testi and Cesaroni 1997; Testi *et al.* 1997; Felli *et al.* 1997).

An excellent example that shows the connection of H_2O and OH masers with the earliest evolutionary phases of YSOs is the work of Torrelles *et al.* (1997) on W75N(B). They observed with the VLA the star-forming region W75N(B) and detected three continuum (at 1.3 cm) sources (VLA 1, VLA 2, and VLA 3) in a region of 1.5 arcseconds. VLA 1 is elongated approximately in the direction of the bipolar molecular outflow. VLA 2 appears unresolved, while VLA 3 shows a bright core plus extended emission. They observed simultaneously the H_2O maser emission toward these sources and detected a total of 29 H_2O maser spots. These masers are mainly distributed in two clusters, one associated with VLA 1 (11 maser spots) and the other one associated with VLA 2 (8 maser spots). Only one maser spot is associated with VLA 3. The masers associated with VLA 1 are distributed along the major axis of the radio jet and are delineating the outflow at scales of 1 arcsecond. The masers coincident with VLA 2 are distributed in a shell and are probably bound.

When the OH maser spots of Baart *et al.* (1986) are plotted in the same Figure as the H_2O masers (see Figure 7 of Torrelles *et al.* 1997), the following picture emerges:

a) The OH and the H_2O masers are close to each other *but never coincident.*

b) No OH maser spot is associated with VLA 3.

c) In VLA 2, there are three OH maser spots, but all of them are further away from the continuum source than the H_2O masers associated with it.

d) In VLA 1, the OH masers (like the H_2O ones) are excited in the jet, but in its outer parts.

The non-coincidence of the OH and H_2O masers is easy to understand theoretically. The H_2O masers thrive in regions where the density is high ($n_{H_2} \sim 10^9$ cm^{-3}). At such high densities the OH molecules are completely thermalized. Nevertheless, the above observations are consistent with the picture that both H_2O and OH masers are pumped in shocks, with the OH masers pumped in less dense regions than the H_2O ones.

The interpretation, in terms of evolution, that Torrelles *et al.* (1997) give is the following: VLA 3 is an ultracompact and less developed H II region. Somewhat more developed is VLA 2, with its associated masers probably tracing bound motions in the surrounding circumstellar gas (rotating disk?). The most developed of all is VLA 1, which exhibits a large-scale molecular outflow. Thus, H_2O masers appear first and then follow the OH masers. This is consistent with the proposal of Forster and Caswell (1989).

8. Conclusions

From the above presentation we hope it has become evident that the astronomical masers are very useful. They are particularly useful in probing the dense star-forming regions. The resolution (μarcsec) achieved with masers cannot be achieved with any other method. Now we have reached the point where several maser lines from the same molecule are observed. This places significant constraints on the theoretical models and for the first time model predictions have been verified observationally. It is also reasonable to expect that maser observations will reveal the physical conditions in the dense parts of star-forming regions.

9. References

Alcock, C., and Ross, R. R. 1985a, *Ap. J.,* **290**, 433.
———. 1985b, *Ap. J.,* **299**, 763.
———. 1986, *Ap. J.,* **306**, 649.
Anderson, N., and Watson, W. D. 1990, *Ap. J.*, **348**, L69.
Andresen, P. 1986, *Astr. Ap.*, **154**, 42.
Baart, E. E., Cohen, R. J., Davies, R. D., Norris, R. P., and Rowland, P. R. 1986, *M.N.R.A.S.*, **219**, 145.
Baudry, A., Desmurs, J. F., Wilson, T. L., and Cohen, R. J. 1997, *Astr. Ap.*, **325**, 255.
Baudry, A., and Diamond, P. J. 1991, *Astr. Ap.*, **247**, 551.
———. 1998, *Astr. Ap.*, **331**, 697.
Baudry, A., Diamond, P. J., Booth, R. S., Graham, D., and Walmsley, C. M. 1988, *Astr. Ap.*, **201**, 105.
Baudry, A., Walmsley, C. M., Winnberg, A., and Wilson, T. L. 1981, *Astr. Ap.*, **102**, 287.
Bloemhof, E. E., Moran, J. M., and Reid, M. J. 1996, *Ap. J.,* **467**, L117.
Bloemhof, E. E., Reid, M. J., and Moran, J. M. 1992, *Ap. J.,* **397**, 500.
Castor, J. I. 1970, *M.N.R.A.S.,* **149**, 111.
Caswell, J. L., and Vaile, R. A. 1995, *M.N.R.A.S.*, **273**, 328.
Cernicharo, J., Thum, C., Hein, H., John, D., Garcia, P., and Mattioco, F. 1990, *Astr. Ap.*, **231**, L15.
Cesaroni, R., and Walmsley, C. M. 1991, *Astr. Ap.*, **241**, 537.
Chapman, J. M., and Cohen, R. J. 1986, *M.N.R.A.S.*, **220**, 513.
Cheung, A. C., Rank, D. M., Townes, C. H., Thornton, D. D., and Welch, W. J. 1969, *Nature*, **221**, 626.
Claussen, M. J., Wilking, B. A., Benson, P. J., Wootten, A., Myers, P. C., and Terebey, S. 1996, *Ap. J. Suppl.*, **106**, 111.
Clegg, A. W., and Cordes, J. M. 1991, *Ap. J.*, **374**, 150.
Codella, C., and Felli, M. 1995, *Astr. Ap.*, **302**, 521.

Codella, C., Felli, M., and Natale, V. 1996, *Astr. Ap.*, **311**, 971.
Codella, C., Felli, M., Natale, V., Palagi, F., and Palla, F. 1994, *Astr. Ap.*, **291**, 261.
Codella, C., Palumbo, G. G. C., Pareschi, G., Scappini, F., Caselli, P., and Attolini, M. R. 1995, *M.N.R.A.S.*, **276**, 57.
Codella, C., Testi, L., and Cesaroni, R. 1997, *Astr. Ap.*, **325**, 282.
Cohen, R. J., Baart, E. E., and Jonas, J. L. 1988, *M.N.R.A.S.*, **231**, 205.
Cohen, R. J., Masheder, M., and Walker, R. N. F. 1991, *M.N.R.A.S.*, **250**, 611.
Deguchi, S., and Watson W. D. 1986a, *Ap. J.*, **300**, L15.
———. 1986b, *Ap. J.*, **302**, 750.
———. 1989, *Ap. J.*, **340**, L17.
———. 1990, *Ap. J.*, **354**, 649.
Deguchi, S., Watson, W. D., and Western, L. R. 1986, *Ap. J.*, **302**, 108.
Desmurs, J. F., and Baudry, A. 1998, *Astr. Ap.*, **340**, 521.
Desmurs, J. F., Baudry, A., Wilson, T. L., Cohen, R. J., and Tofani, G. 1998, *Astr. Ap.*, **334**, 1085.
Doel, R. C., Gray, M. D., and Field, D. 1990, *M.N.R.A.S.*, **244**, 504.
Draine, B. T., Roberge, W. G., and Dalgarno, A. 1983, *Ap. J.*, **264**, 485.
Elitzur, M. 1982, *Rev. Mod. Phys.*, **54**, 1225.
———. 1990a, *Ap. J.*, **363**, 628.
———. 1990b, *Ap. J.*, **363**, 638.
———. 1991, *Ap. J.*, **370**, 407.
———. 1992a, *Astronomical Masers*, (Dordrecht: Kluwer).
———. 1992b, *Ann. Rev. Astr. Ap.*, **30**, 75.
———. 1993, *Ap. J.*, **416**, 256.
———. 1995, *Ap. J.*, **440**, 345.
———. 1996, *Ap. J.*, **457**, 415.
Elitzur, M., Hollenbach, D. J., and McKee, C. F. 1989, *Ap. J.*, **346**, 983.
Felli, M., Testi, L., Valdettaro, R., and Wang, J.-J. 1997, *Astr. Ap.*, **320**, 594.
Fiebig, D., Duschl, W. J., Menten, K. M., and Tscharnuter, W. M. 1996, *Astr. Ap.*, **310**, 199.
Fiebig, D., and Güsten, R. 1989, *Astr. Ap.*, **214**, 333.
Forster, J. R., and Caswell, J. L. 1989, *Astr. Ap.*, **213**, 339.
Gardner, F. F., and Martin-Pintado, J. 1983, *Astr. Ap.*, **121**, 265.
Gardner, F. F., and Whiteoak, J. B. 1983, *M.N.R.A.S.*, **205**, 297.
Gardner, F. F., Whiteoak, J. B., and Palmer, P. 1987, *M.N.R.A.S.*, **225**, 469.
Gaume, R. A., and Mutel R. L. 1987, *Ap. J. Suppl.*, **65**, 193.
Genzel, R., and Downes, D. 1977, *Astr. Ap. Suppl.*, **30**, 145.

Genzel, R., Reid, M. J., Moran, J. M., and Downes, D. 1981a, *Ap. J.*, **244**, 884.

Genzel, R., Downes, D., Schneps, M. J., Reid, M. J., Moran, J. M., Kogan, L. R., Kostenko, V. I., Matveyenko, L. I., and Ronnang, B. 1981b, *Ap. J.*, **247**, 1039.

Goldreich, P., and Keeley, D. A. 1972, *Ap. J.,* **174**, 517.

Goldreich, P., Keeley, D. A., and Kwan, J. Y. 1973, *Ap. J.*, **179**, 111.

Goldreich, P., and Kwan, J. 1974, *Ap. J.,* **190**, 27.

Gray, M. D., Doel, R. C., and Field, D. 1991, *M.N.R.A.S.*, **252**, 30.

Gray, M. D., Field, D., and Doel, R. C. 1992, *Astr. Ap.*, **262**, 555.

Guilloteau, S., Baudry, A., Walmsley, C. M., Wilson, T. L., Winberg, A. 1984, *Astr. Ap.*, **131**, 45.

Gwinn, C. R., Moran, J. M., and Reid, M. J. 1992, *Ap. J.*, **393**, 149.

Herrnstein, J. R., Greenhill, L. J., and Moran J. M. 1996, *Ap. J.*, **468**, L17.

Hofner, P., and Churchwell, E. 1996, *Astr. Ap. Suppl.*, **120**, 283.

Kaufman, M. J., and Neufeld, D. A. 1996, *Ap. J.*, **456**, 250.

Knowles, S. H., Caswell, J. L., and Goss, W. M. 1976, *M.N.R.A.S.*, **175**, 537.

Kylafis, N. D., and Norman, C. 1986, *Ap. J.*, **300**, L73.

———. 1987, Ap. J., **323**, 346.

———. 1990, Ap. J., **350**, 209.

———. 1991, Ap. J., **373**, 525.

Kylafis, N. D., and Pavlakis, K. G. 1992, *Ap. J.*, **400**, 344.

Lekht, E. E., Mendoza-Torres, E., and Sorochenko, R. L. 1995, *Ap. J.*, **443**, 222.

Meehan, L. S. G., Wilking, B. A., Claussen, M. J., Mundy, L. G., and Wootten, A. 1998, *A. J.*, **115**, 1599.

Melnick, G. J., Menten, K. M., Phillips, T. G., and Hunter, T. 1993, *Ap. J.,* **416**, L37.

Menten, K. M., Melnick, G. J., and Phillips, T. G. 1990, *Ap. J.,* **350**, L41.

Menten, K. M., Melnick, G. J., Philips, T. G., and Neufeld, D. A. 1990, *Ap. J.*, **363**, L27.

Menten, K. M., Reid, M. J., Eckart, A., and Genzel, R. 1997, *Ap. J.*, **475**, L111.

Migenes, V., Cohen, R. J., and Brebner, G. C. 1992, *M.N.R.A.S.,* **254**, 501.

Miyoshi, M., Moran, J., Herrnstein, J., Greenhill, L., Nakai, N, Diamond, P., and Inoue, M. 1995, *Nature,* **373**, 127.

Moran, J. M. 1989, in *Handbook of Laser Science and Technology*, ed. M. J. Weber.

Moran, J. M., Reid, M. J., Lada, C. J., Yen, J. L., Jonston, K. J., and Spencer, J. H. 1978, *Ap. J.*, **224**, L67.

Nedoluha, G. E., and Watson, W. D. 1990a, *Ap. J.,* **354**, 660.

———. 1990b, *Ap. J.,* **361**, 653.
———. 1990c, *Ap. J.*, **361**, L53.
———. 1994, *Ap. J.*, **423**, 394.
Neufeld, D. A., and Melnick, G. J. 1990, *Ap. J.*, **352**, L9.
———. 1991, *Ap. J.,*, **368**, 215.
Offer, A. R., van Hemert, M. C., and van Dishoeck, E. F. 1994, *J. Chem. Phys.*, **100**, 362.
Palla, F., Cesaroni, R., Brand, J., Caselli, P., Comoretto, G., and Felli, M. 1993, *Astr. Ap.*, **280**, 599.
Palma, A., Green, S., DeFrees, D. J., and McLean, A. D. 1988, *Ap. J. Suppl.,* **68**, 287.
Palmer, P., Gardner, F. F., and Whiteoak, J. B. 1984, *M.N.R.A.S.*, **211**, 41p.
Palumbo, G. G. C., Scappini, F., Pareschi, G., Codella, C., Caselli, P., and Attolini, M. R. 1994, *M.N.R.A.S.*, **266**, 123.
Pavlakis, K. G., and Kylafis, N. D. 1996a, *Ap. J.*, **467**, 292.
———. 1996b, *Ap. J.*, **467**, 300.
———. 1996c, *Ap. J.*, **467**, 309.
———. 1999, *Ap. J.*, submitted.
Reid, M. J., and Moran, J. M. 1981, *Ann. Rev. Astr. Ap.*, **19**, 231.
———. 1988, in *Galactic and Extragalactic Radio Astronomy,* eds. G. L. Verschuur and K. I. Kellerman, (New York: Springer-Verlag), p. 255.
Reid, M. J., Schneps, M. H., Moran, J. M., Gwinn, C. R., Genzel, R., Downes, D., and Ronnang, B. 1987, in *Star Formation*, eds. M. Peibert and J. Jugaku, IAU Symposium 115 (Dordrecht: Reidel).
Reid, M. J., and Silverstein, E. M. 1990, *Ap. J.,* **361**, 483.
Schneps, M., Lane, A. P., Downes, D., Moran, J. M., Genzel, R., and Reid, M. J. 1981, *Ap. J.*, **249**, 124.
Smits, D. P. 1994, *M.N.R.A.S.*, **269**, L11.
Sobolev, V. V. 1960, *Moving Envelopes of Stars*, (Cambridge: Harvard University Press).
Strelnitskij, V. S. 1984, *M.N.R.A.S.,* **207**, 339.
Testi, L., Felli, M., Omont, A., Perault, M., Seguin, P., Comoretto, G., and Gilmore, G. 1997, *Astr. Ap.*, **318**, L13.
Torrelles, J. M., Gomez, J. F., Rodriguez, L. F., Curiel, S., Anglada, G., and Ho, P. T. P. 1998, *Ap. J.*, **505**, 756.
Torrelles, J. M., Gomez, J. F., Rodriguez, L. F., Curiel, S., Ho, P. T. P., and Garay, G. 1996, *Ap. J.*, **457**, L107.
Torrelles, J. M., Gomez, J. F., Rodriguez, L. F., Ho, P. T. P., Curiel, S., and Vazquez, R. 1997, *Ap. J.*, **489**, 744.
Turner, B. E., Palmer, P., and Zuckerman, B. 1970, *Ap. J.*, **160**, L125.
Wallin, B. K., and Watson, W. D. 1997, *Ap. J.*, **481**, 832.

Watson, W. D. 1994, *Ap. J.*, **424**, L37.
Western, L. R., and Watson, W. D. 1983a, *Ap. J.*, **268**, 849.
———. 1983b, *Ap. J.*, **274**, 195.
———. 1983c, *Ap. J.*, **275**, 195.
———. 1984, *Ap. J.*, **285**, 158.